

ElectroRing: Subtle Pinch and Touch Detection with a Ring

Wolf Kienzle*
wkienzle@fb.com
FRL Research
Redmond, WA, USA

Eric Whitmire*
ewhitmire@fb.com
FRL Research
Redmond, WA, USA

Chris Rittaler
crittaler@fb.com
FRL Research
Redmond, WA, USA

Hrovje Benko
benko@fb.com
FRL Research
Redmond, WA, USA

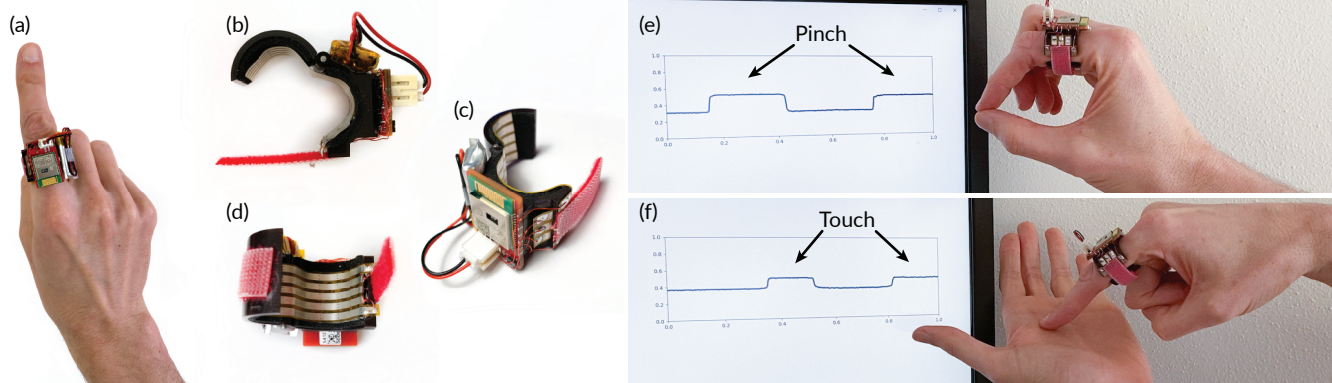


Figure 1: (a) ElectroRing prototype worn on the index finger. (b, c) ElectroRing’s 3D-printed shell with red Velcro strap, red circuit board with shielded microcontroller/Bluetooth module, and Lithium-polymer battery. (d) Electrodes for touch detection placed on the inside of the ring. (e) Real-time plot of raw touch sensor readings while user performs pinch gestures (f) Raw touch sensor readings while user touches their opposite palm.

ABSTRACT

We present *ElectroRing*, a wearable ring-based input device that reliably detects both onset and release of a subtle finger pinch, and more generally, contact of the fingertip with the user’s skin. *ElectroRing* addresses a common problem in ubiquitous touch interfaces, where subtle touch gestures with little movement or force are not detected by a wearable camera or IMU. *ElectroRing*’s active electrical sensing approach provides a step-function-like change in the raw signal, for both touch and release events, which can be easily detected using only basic signal processing techniques. Notably, *ElectroRing* requires no second point of instrumentation, but only the ring itself, which sets it apart from existing electrical touch detection methods. We built three demo applications to highlight the effectiveness of our approach when combined with a simple IMU-based 2D tracking system.

CCS CONCEPTS

• Human-centered computing → Interaction devices.

*Both authors contributed equally to this research.

Permission to make digital or hard copies of all or part of this work for personal or classroom use is granted without fee provided that copies are not made or distributed for profit or commercial advantage and that copies bear this notice and the full citation on the first page. Copyrights for components of this work owned by others than the author(s) must be honored. Abstracting with credit is permitted. To copy otherwise, or republish, to post on servers or to redistribute to lists, requires prior specific permission and/or a fee. Request permissions from permissions@acm.org.

CHI ’21, May 8–13, 2021, Yokohama, Japan

© 2021 Copyright held by the owner/author(s). Publication rights licensed to ACM.

ACM ISBN 978-1-4503-8096-6/21/05...\$15.00

<https://doi.org/10.1145/3411764.3445094>

KEYWORDS

smart ring; touch detection; mixed-reality

ACM Reference Format:

Wolf Kienzle, Eric Whitmire, Chris Rittaler, and Hrovje Benko. 2021. *ElectroRing: Subtle Pinch and Touch Detection with a Ring*. In *CHI Conference on Human Factors in Computing Systems (CHI ’21)*, May 8–13, 2021, Yokohama, Japan. ACM, New York, NY, USA, 12 pages. <https://doi.org/10.1145/3411764.3445094>

1 INTRODUCTION

Increased user mobility requires new ways to interact with computers beyond touchscreens, mice, and keyboards. One promising strategy is to appropriate the user’s skin for touch input [16, 17, 52]. For example, in an augmented reality (AR) application, a user could press a virtual button on their open palm or on their forearm. Besides being always available, the skin as an input surface offers tactile and proprioceptive feedback, which can provide an additional sense of agency. Unfortunately, the effectiveness of this approach hinges on robust, low-latency touch detection, which is challenging to implement with small, unobtrusive sensors that can be worn all day without encumbering the user [52].

Here we present *ElectroRing* (Figure 1), an always-available, wearable input device for touch contact detection on the user’s skin. *ElectroRing* uses an active electrical sensing approach, similar to [52, 55]. Compared to cameras or IMUs (inertial measurement units), this electrical approach has the advantage of providing a step-function-like change in the sensor output on both touch and release, even for subtle gestures. Because *ElectroRing* focuses on detection of the precise moment of touch, rather than *what* or *where*

the user touched, we envision ElectroRing as an ideal companion device for an interactive system like AR glasses, which typically cannot detect subtle or occluded touch gestures using only head mounted cameras [52].

A challenge with the active electrical approach [52, 55] is that it requires two points of instrumentation on the body (transmitter and receiver). To our knowledge, ElectroRing is the first solution that requires only a *single* point of instrumentation. To detect touch, two electrodes on the inside of the ring couple an AC signal onto the user’s finger, and two further electrodes—shielded from the transmitter—detect the small portion of the signal that flows through the finger into the touched surface (Figure 1e, 1f). The ring is battery-powered and transmits data wirelessly to a host application. It also features an on-board accelerometer and a gyroscope—not for touch detection, but to track the ring’s position in our example applications.

In comparison to prior work, ElectroRing combines a number of desirable properties. First, the fingertip is left un-instrumented, and no other points of instrumentation are required (e.g., no accompanying wristband). Second, the signal-to-noise ratio (SNR) of the raw touch signal (Figure 1e, 1f) is substantial (25 dBV) and largely independent of gesture velocity or mechanical impact at contact. This is in contrast to cameras or IMU based solutions, which often require an unnatural range of motion or forceful contact to detect touches reliably. Third, ElectroRing detects both touch *and* release events, a requirement for rich user interfaces with 2-state transactions, such as drag & drop or inking [4].

The contributions of our work are:

- The design of a ring that electrically senses subtle touch and release events on the user’s skin, using a *single* point of instrumentation
- A characterization of the raw touch signal vs. gesture intensity and an evaluation of an end-to-end pinch and palm-touch detection system
- Three example applications that combine the ring’s touch sensor with its on-board IMU to highlight possible implementations of a fully functioning input device.

2 RELATED WORK

ElectroRing provides precise touch segmentation, which is a critical piece of the long-standing research vision of enabling on-demand computing surfaces [16, 33, 44]. Alternatives to appropriating everyday surfaces for touch input include the use of explicit touch surfaces on personal computing devices like smartphones, smart watches, or head-mounted displays [23, 25], or the instrumentation of environmental objects with optical [1, 15, 26], acoustic [28, 30, 31], electric impedance tomography [49, 51, 53], or capacitive [8, 9, 24, 42, 54] sensors. We focus the remainder of this section on wearable sensors that scale to new environments. Specifically, we review prior work on touch detection with camera-based systems, capacitive sensors, systems that instrument the wrist, and systems that instrument the finger.

2.1 Camera-based Systems

Egocentric cameras are an attractive solution to ubiquitous touch input due to the potential to solve both touch segmentation and

touch localization in one device. The proliferation of commodity depth cameras, such as the Microsoft Kinect, has made this problem much more tractable. For example, OmniTouch [16], uses a wearable depth camera and projector system to turn everyday body and world surfaces into interactive touch surfaces. Touch detection is realized using image processing techniques on a depth map and results in about 1 cm to 2 cm of ambiguity in touch contact. MRTouch [45] improves on this work using the refined depth sensing system in a Microsoft HoloLens, but still suffers from touch ambiguity at close distances.

Because ElectroRing uses an electrical sensing technique, it is not based on the finger’s height above the surface; instead, it offers performance more similar to widely used capacitive touch surfaces, which allow very subtle and precisely timed touches. We argue that such touch precision is essential to enabling robust interfaces that give users confidence.

2.2 Capacitive Sensing

Capacitive sensing is one of the most ubiquitous methods of detecting precise touch between a user and an interactive device with high SNR. Beyond its frequent use for touch detection in devices like smartphones, watches, and tabletop surfaces, recent advances have enabled new kinds of interaction techniques. DiamondTouch [8, 9] and similar efforts [18, 42] show how capacitive sensing can be used to capture user and object identity. Touché uses swept-frequency capacitive sensing to detect both touch and gestures [35]. Other devices instrument on-body touch surfaces through wearable fingertip devices [46], clothing [34], or touchable tattoos [19, 29, 43]. A common feature of these systems is the need for instrumentation at the touch interface. ElectroRing detects touch between the fingertip and the body without any instrumentation of the touch surface. Instead, a more conveniently placed ring remotely detects when the fingertip has made contact with the skin.

ElectroRing is most similar to an active capacitive sensing system operating in both transmit and receive mode, sometimes called intrabody coupling [12]. However, it would be more accurately described as a galvanic intrabody system. Unlike most capacitive systems, ElectroRing’s electrodes are fixed to the skin and the capacitance between the electrodes and user does not change. ElectroRing remotely senses touch events by measuring the current between differential receive electrodes.

2.3 Instrumented Wrists

Touch contact can be detected through electrical, inertial, or acoustic sensors embedded in a wristband. ElectroRing is most similar to the active electrical touch detection techniques demonstrated in SkinTrack [55] and ActiTouch [52]. SkinTrack [55] uses a ring that couples an 80 Mhz AC signal to the body and a wristband on the opposing arm to detect the presence and location of the fingertip as it touches the palm. Although ElectroRing does not attempt to detect touch location, it is capable of detecting touch state with just a single point of instrumentation. ActiTouch uses a similar technique to couple a signal to the user’s wrist and measure the signal flow through the body on a head-mounted device. Although the sensing principle is similar, ElectroRing eliminates the need

for head or wrist instrumentation by directly measuring the signal flow in the same device.

Other wristbands or armbands use acoustic [17] or inertial methods [50] to detect touch. These techniques are limited to on-body touches and require significant tap force. Moreover, these methods are incapable of detecting release events. Mujibiya et al. [27] demonstrate an ultrasound-based technique using an armband and a ring to detect touch state and location. ElectroRing’s electrical approach requires only a single point of instrumentation.

2.4 Instrumented Fingers

A variety of sensing techniques have been explored in rings and other finger-mounted form-factors to enable interaction in mobile scenarios. Miniature cameras have been embedded in rings to support hand tracking [5], to read text for users with visual impairments [3, 37], or to understand the user’s context of interaction [36, 47]. Magic Finger [47] uses a fingertip-mounted camera to detect touch and classify surfaces based on texture. In contrast, ElectroRing detects touch in a ring form-factor without covering the fingertip.

Other devices instrument the fingertip to electrically detect touch contact with the thumb. Tip-Tap [20] detects thumb-to-finger gestures without a battery using tattoos containing RFID antennas. TipText uses a capacitive sensing array at the fingertip for subtle text entry using the thumb [46]. While ElectroRing requires a battery and focuses exclusively on touch detection, it offers a more convenient form-factor by leaving the fingertips unencumbered and requiring only a single point of instrumentation in a ring.

Magnetic approaches have been proposed for occlusion-free tracking of the fingertip [6, 7] or a finger-worn ring [2, 32]. However even with precise finger tracking, robust segmentation of touch requires additional sensing. Inertial sensing techniques have been used on the finger for a variety of tracking and pointing tasks [14, 21, 48] as well as touch detection [10, 11, 13]. In this work, we show that ElectroRing can potentially detect lighter touches than inertial techniques and can also detect release events, which is often not feasible with an IMU.

It is worth noting that the touch detection in ElectroRing complements many other sensing and interaction techniques previously demonstrated. In this work, we demonstrate three basic applications using an IMU as the only additional sensor, but richer applications can be realized by combining ElectroRing’s touch detection with, for example, the finger tracking approach in LightRing [21].

3 THEORY OF OPERATION

ElectroRing detects touch state by coupling a 10.7 MHz AC signal to the body and indirectly measuring the signal flow through the finger. This frequency is sufficiently high to conduct well through the body. It is also a standard intermediate frequency used in radio receivers, which makes it easier to find small integrated oscillators and other components that operate in this range. ElectroRing uses two pairs of electrodes: 1) a proximal differential transmit pair that couples the AC signal to the body and 2) a distal differential receive pair that measures the voltage gradient along the finger. A fifth shield electrode between the transmit and receive pairs acts as an AC return path. It improves the signal-to-noise ratio by blocking

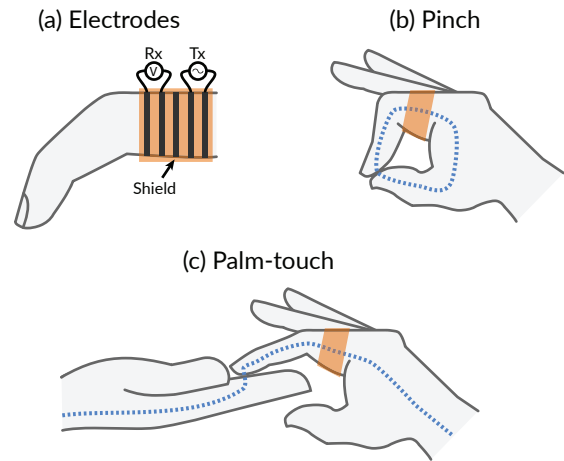


Figure 2: (a) ElectroRing uses five electrodes: two transmit electrodes (closest to the palm) differentially couple the AC signal to the finger, the middle electrode shields direct coupling between the Tx and Rx electrodes, two receive electrodes (distal) measure the gradient of the signal along the finger. (b) During a pinch, the signal travels through the thumb and galvanically back to the transmit electrode. (c) Touching the opposing palm creates a galvanic path through the body back to the proximal transmit electrode.

any fringe fields from the transmit electrodes from directly coupling into the receive electrodes. Figure 2a shows the electrode layout along the finger. When the user pinches or touches their opposing palm, a small current flows in a circuit through the finger, into the touched surface, and back to the ring (Figure 2b, 2c).

ElectroRing uses *differential* transmitter electrodes (shown as Tx in Figure 2a), which means the signal flows from one of the transmitter electrodes back into the other. When in contact with the skin, most of the signal travels through the short path in the body between these two transmitter electrodes. To detect touch, ElectroRing relies on trace current that flows along an electrically parallel path through the body that is formed when the finger makes contact with the thumb or palm. While not touching anything, both receiver electrodes (shown as Rx in Figure 2) measure roughly the same level of the transmitted signal; there is little difference between the two receivers because there is no current flow between them. In contrast, when the user touches their skin, a return path is formed between the touched surface and the proximal transmitter electrode. The flow of current, although small, creates a differential voltage between the two distal receive electrodes, which, with sufficient amplification, can be measured and used as a touch signal.

The path along which the current travels back to the transmit electrode varies depending on the which part of the body is touched. Figure 2b and 2c show the current path for both pinch and palm-touch, respectively. When the user performs a thumb-to-finger pinch, this creates a skin-skin interface which the high-frequency signal can easily cross. The signal then follows a fairly low-impedance galvanic path through the thumb and back to the

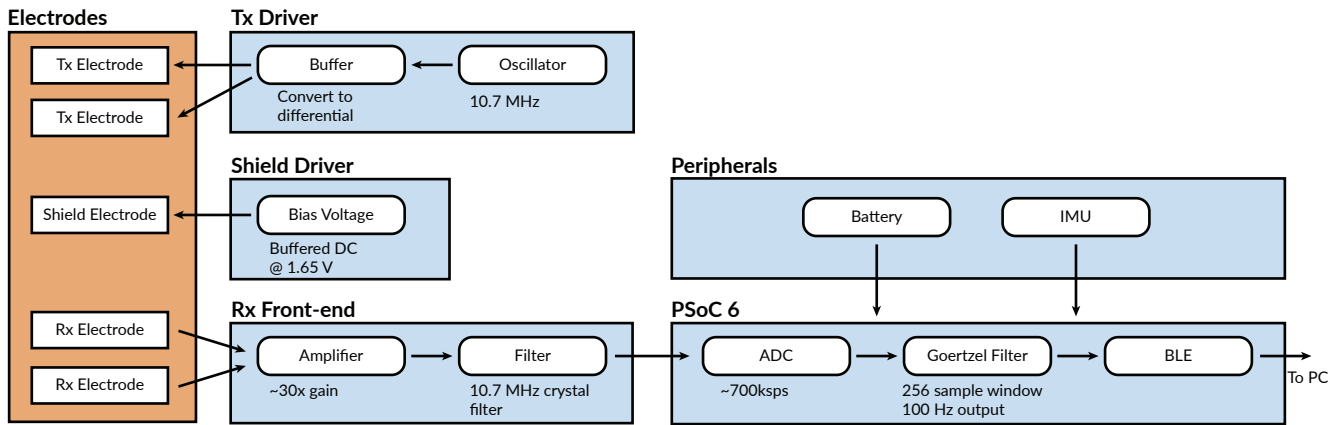


Figure 3: Block diagram of ElectroRing hardware. The transmit driver buffers a 10.7 MHz signal and applies it to the two transmit electrodes. A shield driver holds the shield electrode at a DC voltage. The receive front-end amplifies and filters the signal, which is sampled by an ADC on the PSoC. The PSoC applies a Goertzel filter and streams the values to a PC.

proximal transmit electrode. A touch on the opposing palm also creates a skin-skin interface as well as a galvanic path through the body.

Although proximity of the finger to the thumb or opposing palm does create some capacitive coupling even when not touching, it does not act as an effective proximity sensor and there is a distinct increase in the signal at the moment of physical contact (see Figure 4). While current paths are shown as distinct lines in Figure 2, these are only illustrative. In reality, the body is a complex network of resistive and capacitive components. Additional complexities are introduced at the ring by the tissue-skin and skin-electrode interfaces. However, our simplified body model serves as a helpful guide for reasoning about the properties of ElectroRing. For a more in-depth discussion of electrical body models, we refer the reader to related work in the field of body-coupled communications [38, 39].

This electrical method of touch detection is similar to that of ActiTouch [52], which placed transmit electrodes on a wristband and receive electrodes on a head-mounted display. Simply mounting the two electrode pairs close together on a single device, however, results in saturation of the receiver electrode and poor sensitivity to touch. We were able to sense touch from a single point of instrumentation by introducing an additional shield electrode between the transmit and receive electrodes, optimizing the receiver amplifier topology, and moving the device closer to the fingertip.

4 HARDWARE

ElectroRing consists of 1) a small, battery-powered printed circuit board (PCB) that handles signal generation, measurement, and communication, 2) five electrodes that contact the finger, and 3) a mechanical enclosure in a ring form-factor. Figure 3 shows a system-level overview. For detailed schematics, refer to the appendix. On the PCB, the 10.7 MHz square wave signal is generated by a MEMS oscillator (DSC6003). A unity-gain buffer and inverting amplifier (dual OPA2836) converts the signal from single-ended to differential. This 3.3 V differential output is capacitively coupled to the two transmitter electrodes. The two receive electrodes are amplified

with 30 times gain and converted to a single-ended signal using an instrumentation amplifier (3x LTC6253). The signal is then filtered using a narrow-band ceramic filter and buffered for sampling by an ADC.

A Cypress PSoC 6 system-on-chip handles data acquisition, touch state detection, and communication with a PC over BLE. The receive signal is under-sampled by the on-board ADC at approximately 700 ksp. A firmware algorithm detects the amplitude of the aliased 10.7 MHz signal using a software Goertzel filter with 256 samples. The exact sampling frequency was optimized to minimize frequency spreading and maximize the signal power in a single frequency bin. Because the hardware ceramic filter has narrow bandwidth, there is little other noise that could alias into the measured frequency band.

The data sampling is duty-cycled and the data rate can be controlled depending on application needs. In this work, the data rate was fixed to 100 Hz. For data collection purposes, the raw signal was streamed over BLE to a host PC for processing and logging. To minimize BLE communication overhead, the entire algorithm can also be implemented in firmware, so that only discrete touch events need to be sent over BLE. ElectroRing also contains an on-board IMU to enable applications that require positional tracking for pointing or swiping. For the purpose of this paper, all IMU data was streamed over BLE and processed on a PC.

ElectroRing is implemented on a custom PCB that measures 27 mm by 17 mm. It is powered by a small 407 mWh lithium polymer battery affixed to the side of the ring. Overall, the system consumes approximately 220 mW of power (for a lifetime of 1-2 hours). However, we note that this system is currently optimized for flexibility and not power consumption. Initial efforts to reduce power through hardware optimization and duty-cycling the measurements has yielded a device that consumes just 18.5 mW (approximately 22 hours continuous operation on the same battery) with no noticeable degradation in signal quality.

To maximize fit across users and make it easier to don, the ring consists of two 3D-printed shells, connected by a hinge on one side

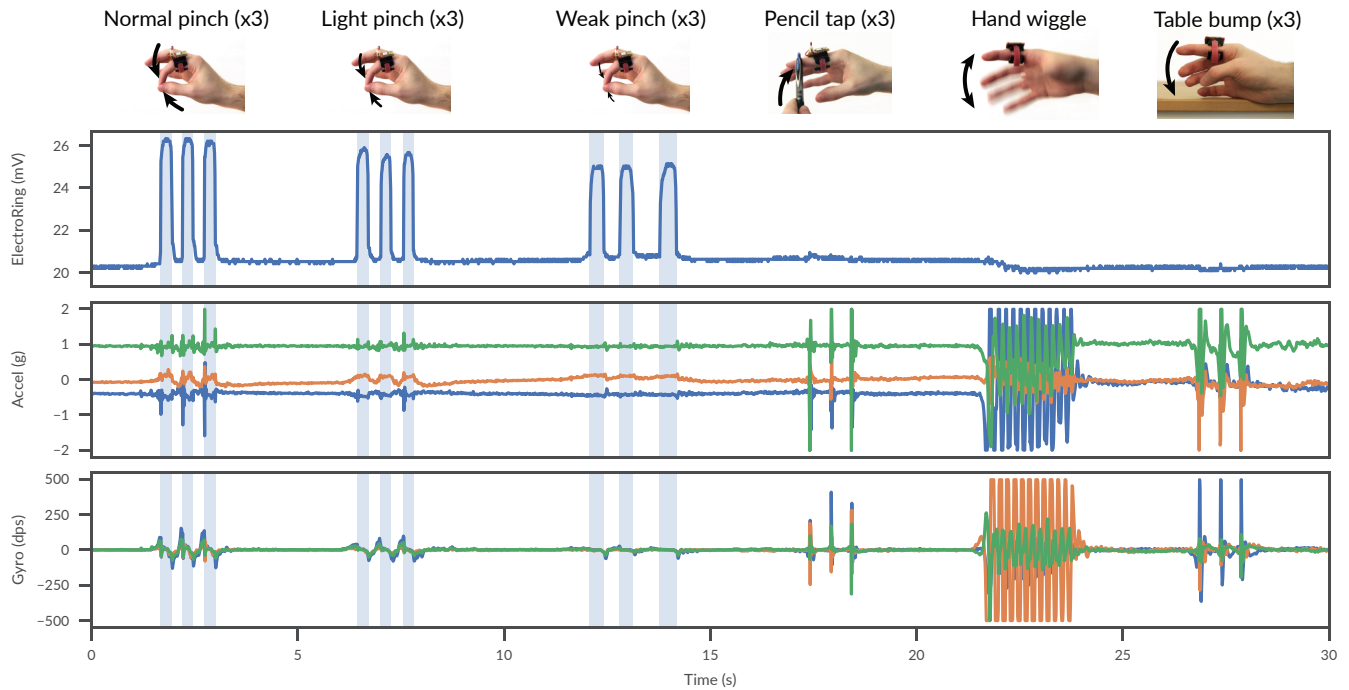


Figure 4: Raw touch sensor (top), accelerometer (middle), and gyroscope (bottom) data for six different activities as function of time: normal pinch, light pinch, weak pinch, and three non-touch distractor activities. Pinch states are shown as shaded vertical bars. Note how subtly the third set of pinches was performed—peak acceleration (middle plot) and angular velocity (bottom plot) during these "weak" pinches are close to noise level.

and Velcro on the other (Figure 1b). The hinge allows the ring to swing open and closed to fit the user’s finger and the Velcro strap ensures a snug fit. The interior surface of the ring is covered with a thin layer of foam for comfort. The electrodes are printed on a flex circuit board using a copper conductor with tin plating and are attached to the foam lining with double-sided tape.

The exact size and spacing between the electrodes can be adjusted depending on the user’s finger and application requirements. In this work, we built two rings, which performed comparably: one with 2 mm wide electrodes, and one with 3 mm wide electrodes. Both rings had 1 mm gaps between electrodes, leading to an overall electrode width of 14 mm and 19 mm, respectively. The corresponding 3D-printed ring shells are 15 mm and 20 mm wide, respectively.

5 SIGNAL PROCESSING

Before designing the touch detection algorithm, we visually inspected the raw signal from the touch sensor for different activities as shown in Figure 4. The top plot shows the output of the Goertzel filter in mV. The plots below show unfiltered readings from the on-board accelerometer and gyroscope, respectively. The sampling rate for all three plots was 100 Hz.

An initial observation from Figure 4 is that touch states—denoted by the shaded vertical bars—clearly stand out visually in the raw ElectroRing touch signal. At touch/release events, the signal

rises/falls very quickly, typically between 10% and 90% from one sample to the next at 100 Hz. Notably, the touch signal level during touch states is largely independent of 1) the impact of the fingertip coming into contact with the surface—indicated by a sharp peak in the accelerometer reading, and 2) the angular velocity of the finger during the gesture (amplitude of the gyroscope signal).

The second half of the time series in Figure 4 shows that the raw touch signal is quite robust to finger motion that is *not* related to a touch gesture, but clearly registers on the IMU, and could lead to false detections in an IMU-based touch detector. Finally, we observe some baseline drift in the touch signal, but it is slow and small compared to the signal change at touch and release events.

To further characterize how the touch signal varies with gesture type and intensity, we recorded five short pinches and palm touches from an expert user at three subjective intensity levels: "normal", "light", and "weak". The two bottom graphs in Figure 4 show an example of IMU readings vs. subjective intensity level, with amplitudes decreasing from "normal" to "light" to "weak". Here, "weak" refers to a touch in which an effort was made to make contact as gently as possible while exerting no force. We computed the signal-to-noise ratio (SNR) of each touch event as described in Equation 1.

$$\text{SNR} = 20 \log_{10} \left(\frac{\text{mean}(v_{\text{touch}}) - \text{mean}(v_{\text{no-touch}})}{\text{std}(v_{\text{noise}})} \right) \quad (1)$$

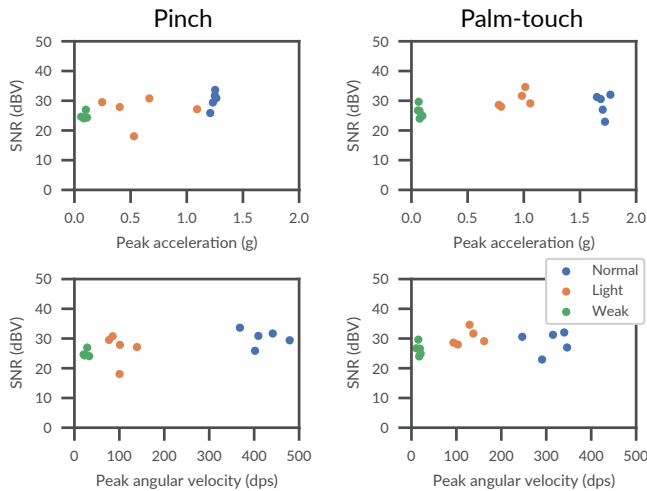


Figure 5: Scatter plots of ElectroRing SNR for pinch and palm touch gestures vs. intensity as measured by accelerometer (top row) and gyro (bottom row). Color represents gesture intensity as intended by the user during the recording. For both pinch and palm touch, SNR values are consistently around 25 dBV, even for the weakest gestures (green), where the finger moved extremely slowly, below 10 dps and 0.1 g.

v_{touch} are samples from a touch segment, $v_{\text{no-touch}}$ are samples from a non-touch segment, and v_{noise} are samples from the preceding non-touch segment. We also computed the peak acceleration and peak angular velocity around each touch event as a measure of gesture intensity (for acceleration, a 1-second moving average was subtracted to remove the effect of gravity). Figure 5 shows SNR consistently around 25 dBV for both pinch and palm touch, and essentially independent of gesture intensity. This suggests that we can robustly detect very subtle pinches and touches.

Motivated by these observations, we implemented a simple touch detection algorithm (Figure 6): we first remove the high frequency noise with a 3-tap median filter (30 ms window at 100 Hz sample rate). Then, we compute the signal change between the current and previous sample. If the signal change is greater than a threshold, we report a *touch* event. If the change is less than a second (negative) threshold, we report a *release* event. The two touch thresholds were tuned on a small training data set, as described in the next section. The algorithm keeps track of the current touch state to suppress touch events while in contact, and release events while not in contact. Finally, to de-bounce the detector output, we suppress any touch events closer than 6 samples (60 ms) to the last release.

6 EVALUATION

Due to logistic constraints caused by the COVID-19 pandemic, all experiments were performed in the two first authors’ homes, and by the authors only. While this left us with a small number of test subjects, which have to be considered experts, we believe that the generality of our results is supported by two beneficial effects. First, we used two hardware prototypes that were assembled separately

by each author in their respective homes (except the PCB) and should exhibit some variation in their function. Second, our signal processing algorithm is extremely simple, with only a small number of parameters.

We collected pinch and palm touch data from two of the authors over 5 days with 2 sessions per day. Each session consisted of 10 light pinches and 10 light palm touches. The first 5 pinches/touches within a session were short taps, about one second apart. The second 5 pinches/touches were performed with drag/swipe motion during contact. This yielded a total of 400 touch and release events, which were manually annotated by marking the half-way point in each touch/release ramp in raw touch signal. The average length of a touch state was 322 ms (SD 229 ms) and the average length of a no-touch state was 415 ms (SD 293 ms). We used data from the first session (the first 10 pinch and 10 tap events from both users, i.e., 40 events total) to tune the two thresholds in our algorithm, and the remaining data (9 sessions, both users) to evaluate the resulting system’s accuracy.

To tune the touch and release threshold in our algorithm, we searched over a two-dimensional grid of possible thresholds (in mV), minimizing the total number of false touches/releases and missed touches/releases. A detection was counted as false or missed if it occurred more than 80 ms before or after the true (manually annotated) event time. The search range was set to 0 mV to 3 mV for touch, and -3 mV to 0 mV for release, in steps of 0.1 mV. This yielded optimal thresholds of 1.1 mV for touch and -0.7 mV for release. We evaluated the detector on the remaining 18 sessions (360 touch/release events) from the two users. We counted only two errors overall (0.6%): one missed pinch onset for one user, and one early palm touch release for the other user. The threshold search was performed *once* in this study, *jointly* for all users.

We also measured the latency between true event times—as manually labeled in the raw data—and detected events returned by our algorithm, not counting downstream BLE communication etc.

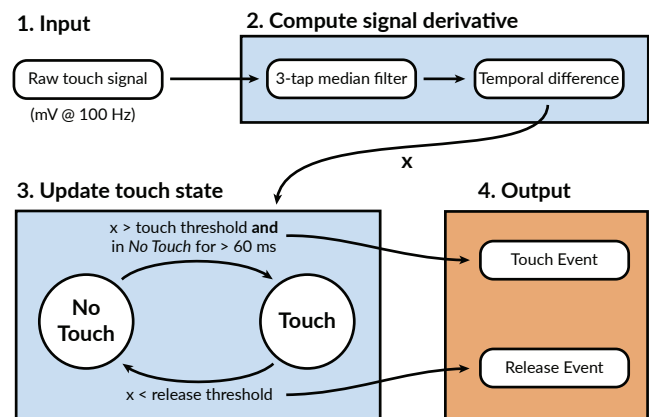


Figure 6: Touch detection pipeline. The raw signals from the ElectroRing hardware are filtered and temporal differences are computed. This signal drives a state machine that detects touch and release events. Simple touch and release thresholds are used to determine state transitions.



Figure 7: ElectroRing’s ability to detect subtle touch/release events with precise timing enables a number of useful applications when combined with a pointing technique such as an IMU: (a) In-air drag & drop using finger pinches. (b) Pinch to segment strokes while drawing in mid-air. (c) Carousel/slider with inertia controlled by taps/swipes on the palm.

Note that due to the electrical sensing approach, the time between a physical touch event and the corresponding ramp in the raw sensor reading should be negligible. In contrast, our detection algorithm may introduce noticeable latency. The 3-tap median filter delays sudden signal level changes by one sample (10 ms) already. Fortunately, our algorithm did not add significantly to that. We measured an average latency of 15 ms (SD 3.0 ms) for touch events and 11 ms (SD 3.1 ms) for release events.

These results highlight the system’s ability to detect touches with high reliability (> 99%) and very low latency (roughly the time of one video frame at 60 Hz), across 18 don/doff sessions, 5 days, and 2 users with different hardware prototypes. As mentioned above, a larger user experiment is required to claim wider generality. However, given the high SNR of the raw signal and the simplicity of the algorithm, we believe that similar performance can be achieved for most users.

7 APPLICATION EXAMPLES

We built three application examples to highlight ElectroRing’s effectiveness: in-air drag & drop, in-air drawing, and navigating a carousel-style date picker (Figure 7).

7.1 Pinch to Drag & Drop

This first demo lets the user drag and drop documents between two lists. Two-dimensional tracking is achieved by integrating rotation rates from the gyroscope (around the yaw and pitch axes, the roll axis was ignored). With an IMU alone, there is no easy way for the user to signal transitions between pointing and dragging states [4]. ElectroRing lets the user indicate dragging vs. pointing state with a subtle pinch gesture. Without reliable detection and precise timing of these state transitions, documents could easily be placed in unwanted slots.

7.2 Pinch to Draw

This example shows an in-air drawing experience. Here, the virtual pen is only drawing while the user is pinching. As in the drag & drop example, the two-dimensional tool position is controlled by integrating two of the gyroscope readings. Inking nicely illustrates the importance of precise timing of pen up vs. pen down transitions; any latency in pinch/release detection or ambiguity in the exact

touch moment would result in strokes that start or end in other locations than intended.

7.3 Palm-touch Carousel

To demonstrate the potential of on-body interfaces we implemented a carousel date picker that is controlled by swiping on the user’s palm. While discrete swipe gestures are easy to detect with inertial sensors, this application shows continuous directional input that enables much richer usage, e.g. for kinetic scrolling. Here, the user can lightly brush the palm surface to drag, quickly swipe to accelerate, or tap and hold to stop (brake) the carousel motion. Left/right motion is derived from the rotation around the vertical gyroscope axis.

Figure 8 illustrates how the carousel application benefits from ElectroRing’s ability to 1) detect subtle touches and 2) report touch and release events with low latency. First, with the fingertip moving fast and mostly parallel to the surface, touch states are typically short and make only light contact. ElectroRing’s SNR is still high in these cases, even when touch or release events are barely visible in the IMU data. Second, touch and release events need to be localized precisely in time. Otherwise the system could misinterpret a direction change at the beginning or end of a swipe as a swipe in the opposite direction.

8 CONTACT WITH OFF-BODY SURFACES

While the primary aim of ElectroRing is to detect on-body touches, we note that it can also detect contact with various conductive surfaces external to the body. As discussed previously, during “normal” on-body operation the body forms a galvanic return path between the fingertip and the proximal transmit electrode (Figure 2). For off-body operation, the conductive environmental surface offers a capacitive return path to the body. This scenario relies on the ever-present capacitive coupling between the human body and various objects in the environment. Figure 9 shows a simplified electrical pathway for touch on a conductive off-body object. If the object touched is electrically grounded, it is likely to trigger a detectable signal change regardless of size. However, ungrounded conductive objects of sufficient size also have enough capacitive coupling to the body to support a reasonable return path.

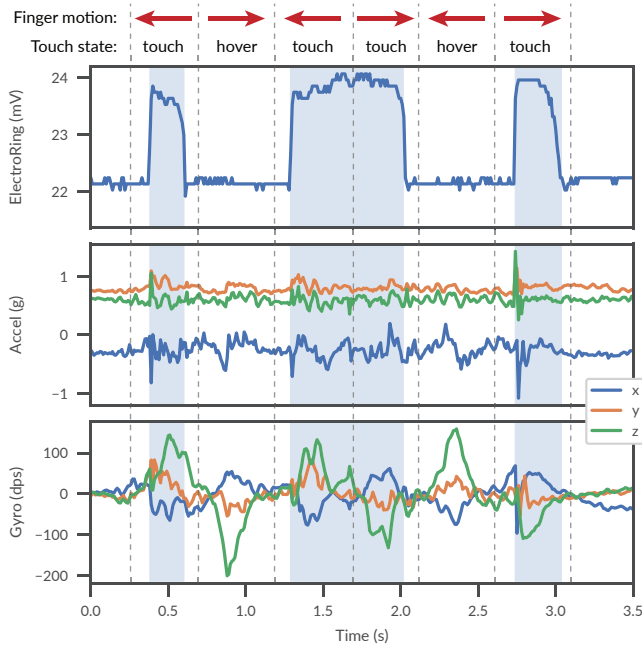


Figure 8: The carousel application (see Figure 7c) requires robust and precisely timed touch and release events in order to determine whether the user’s finger motion occurs while in contact with the palm or while hovering. This figure shows sensor readings during a series of horizontal swipe/drag gestures on the palm: the top graph shows the touch signal and states of contact (shaded areas). The gyro’s vertical axis (green curve, bottom plot) drives the motion of the swipe (also shown as red arrows at the top). The touch signal shows high SNR, even though touch and release events are masked by other motion in the IMU data. Precise temporal segmentation allows ElectroRing to accurately capture fast, complex motions like back and forth swipes on the palm without lifting the finger.

To better understand ElectroRing’s ability to detect contact with various surfaces, we conducted a supplementary evaluation in which we compared the response of on-body surfaces to grounded, conductive, and non-conductive off-body surfaces. One of the authors wore ElectroRing and touched 20 different surfaces five times each. For each surface, the average SNR was computed according to Equation 1.

Figure 10 shows the results from this analysis, grouped by on-body and off-body surfaces. As expected, touching the bare skin of the thumb, palm, or forearm achieves a high signal-to-noise ratio. Touching the body through clothing significantly degrades the signal. For off-body surfaces, large or grounded metal objects, such as a metal table, perform comparably to touches on skin. Conductive objects making contact with another point on the body, such as a metal object held in the hand also perform quite well. As the surface area shrinks or the conductivity degrades, so does the measured

SNR. Most non-conductive objects, such as a wooden table, exhibit no response at all.

While this approach does not lend itself to ubiquitous surface touch interaction [16, 45], it does provide highly robust touch detection on a limited set of conductive surfaces. This could enable various interactions on known objects, such as the surface of a metal table, or provide a method for researchers to prototype such interactions simply by placing a conductive layer, such as aluminum foil, on any surface.

9 DISCUSSION AND FUTURE WORK

ElectroRing robustly detects both touch and release events, in contrast to systems that focus only on touch events [10, 11, 13, 31]. This enables a rich set of two-state interactions, like inking, drag-and-drop, and rubber banding [4], as shown in Figure 7. Moreover, because ElectroRing relies on an electrical detection technique, it supports subtle touches, reducing the burden on users to perform

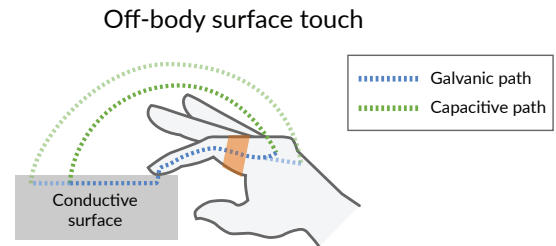


Figure 9: Touching a conductive surface creates a capacitive return path based on the coupling between the surface and the user’s body.

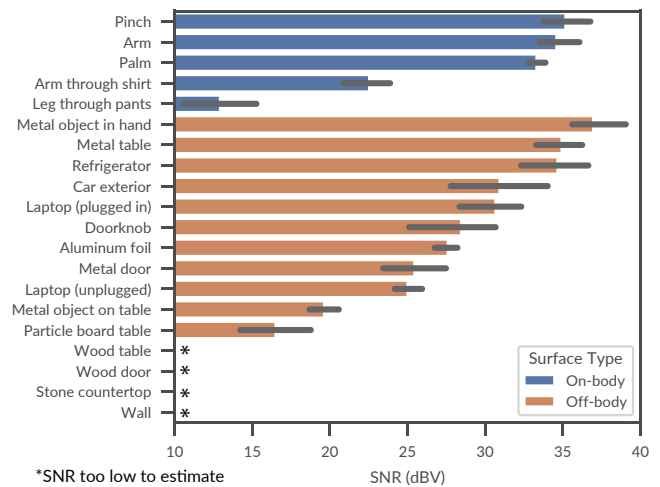


Figure 10: SNR for touches on various on-body and off-body surfaces. Touching bare skin or large conductive objects performs best. Non-conductive objects exhibit poor SNR or are not detectable at all.

deliberate, tiring gestures. For example, when paired with an augmented reality headset, a user might quickly pinch and release without moving their arms to dismiss a notification or pinch and drag on a radial menu to interact with it.

Among prior work, ElectroRing is most similar to ActiTouch [52], which placed electrodes on a head-mounted display and a wristband to detect contact between a fingertip and the opposing palm. Both rely on coupling an AC signal to the body and measuring how the signal changes during a touch event. ElectroRing builds on ActiTouch by moving all instrumentation to a single point on the body (one ring vs a wristband plus headset). This both provides less encumbrance for the user and enables new kinds of interactions that only require a single hand. Specifically, ElectroRing enables thumb-to-finger pinch interactions and touch on certain conductive off-body surfaces.

While these new use cases enable exciting new interaction possibilities, ElectroRing is not capable of differentiating between contact with different surfaces (e.g., thumb, palm, or conductive objects). We envision relying on a complementary sensing method to differentiate between touch surfaces and track touch location. In this work, we used an IMU to highlight several simple use cases, but the use of vision-based hand tracking can enable richer interactions [16, 45, 52]. Future work could also explore whether the use of capacitive coupling techniques common in body channel communications [39] can enable distinguishing between on-body and off-body touches. Another exciting avenue of research is to pair ElectroRing with other wearable techniques for tracking finger motion [14, 21, 22, 32] to more fully capture the state of the hand and finger.

While this work focused on delivering binary detection of touch and release, it may also be possible to detect touch pressure. The amplitude differences in Figure 4 already demonstrate a modest difference in signal amplitude for different touch intensities, which are likely related to the contact area of the touch. We believe it will be challenging to reliably estimate *absolute* pressure this way due to other sources of signal variations of similar or higher amplitude, such as changing electrode/skin impedance caused by small movements of the ring on the finger, that could mask pressure-dependent signal changes. However, tracking relative pressure while the finger is resting on a surface is likely feasible. Future work could also explore the use of frequency sweeps [35] to better characterize the touch pressure or perhaps classify the type of surface touched.

With an overall width of 15 mm to 20 mm, the device is somewhat large for daily use. Future work should explore eliminating the central electrode and optimizing the electrode shape and size. For example, it may be possible to split the electrodes between the palmar and dorsal sides of the finger, reducing overall width. Another potential optimization may be to use other electrode configurations, e.g., a single-ended transmitter, which would use capacitive coupling of the PCB ground as the return path. The use of adjustable velcro straps on the ring made it easy to control the tightness of the band and to ensure comfort during use. While the device does not need to be tight, it is important that the electrodes make contact with the skin, a more difficult task for traditional rigid rings. Future designs could explore techniques to add additional mechanical compliance or deformable electrodes to improve both comfort and contact reliability. Additionally, while there is precedent for

the use of a interactive ring on the index finger [14, 21, 32], additional ergonomic studies are needed to understand the usability and acceptability of this form-factor during extended use. Future work should also consider alternative form-factors for this sensing approach. ElectroRing has such a high SNR because of its proximity to the fingertip, but if a similar technique can be achieved in a single wristband form-factor, it may reduce overall user encumbrance and enable detection of touches by other fingers, not just the instrumented finger.

While we believe this approach will generalize across users, the current evaluation of the system was performed with only two expert users. Future studies should explore how variation among users, especially novice users, impacts performance. Variables like touch technique, hand size, skin conductivity, and hydration may have some effect on the measured signal strength. However, given the high signal-to-noise ratios observed in this work, it is likely that acceptable performance can be achieved even in the most challenging conditions. To reduce the potential for overfitting on data collected from two expert users, we chose an algorithm that is extremely simple, with just two tunable parameters. If suitable defaults cannot be found that fit a large population, these parameters could be personalized through a per-user calibration step, e.g. by guiding users through a initial setup experience or game that prompts them to pinch and tap a number of times after they first set up the device.

ElectroRing uses BLE to communicate data back to a host PC. However, we note that systems that couple an AC signal to the human body have previously been used to transmit data in body-coupled communications [11, 38–41]. By modulating the transmit signal, it may be possible to send ElectroRing data to a wristband or other wearable device with low power and minimal hardware modifications. Even without transmitting data, the system can be duty cycled to save power consumption. Currently, despite continuous signal transmission, the ADC is only active less than 4% of the time. By eliminating BLE transmission and duty cycling the signal conditioning circuitry, we estimate we can reduce power consumption to a level suitable for all-day use.

10 CONCLUSION

In this work, we presented ElectroRing, a ring that uses an electrical technique for measuring the precise moment of contact and release between the fingertip and the user’s skin. Unlike previous implementations of this technique, ElectroRing requires only a *single* point of instrumentation on the body. By coupling a signal to the fingertip and measuring how the signal gradient changes with touch, ElectroRing can robustly detect even subtle finger pinches or touch contacts with the opposite palm. Not only does this enable on-body interfaces, which provide tactile and proprioceptive cues, but the degree of precision in ElectroRing’s touch segmentation enables high-fidelity touch interfaces with capabilities beyond what can be achieved with inertial or computer-vision techniques alone. We also demonstrated how ElectroRing can be used to detect contact with certain conductive off-body surfaces, like a metal table. This work has the potential to bridge the gap between the deliberate, discrete input common in wearable devices and the expressive, low-effort interactions afforded by modern touch screens.

ACKNOWLEDGMENTS

The authors would like to thank Josh Weiber for his help on the mechanical design of the ring, and Neil Weiss, Roger Boldu, and Shiu Ng for insightful discussions on the sensing principle and applications.

REFERENCES

- [1] A. Agarwal, S. Izadi, M. Chandraker, and A. Blake. 2007. High Precision Multi-touch Sensing on Surfaces using Overhead Cameras. In *Second Annual IEEE International Workshop on Horizontal Interactive Human-Computer Systems (TABLETOP'07)*. 197–200.
- [2] Daniel Ashbrook, Patrick Baudisch, and Sean White. 2011. NENYA: Subtle and Eyes-Free Mobile Input with a Magnetically-Tracked Finger Ring. In *Proceedings of the SIGCHI Conference on Human Factors in Computing Systems* (Vancouver, BC, Canada) (CHI '11). Association for Computing Machinery, New York, NY, USA, 2043–2046. <https://doi.org/10.1145/1978942.1979238>
- [3] Roger Boldu, Alexandru Dancu, Denys J.C. Matthies, Thisum Buddhika, Shamane Siriwardhana, and Suranga Nanayakkara. 2018. FingerReader2.0: Designing and Evaluating a Wearable Finger-Worn Camera to Assist People with Visual Impairments While Shopping. *Proc. ACM Interact. Mob. Wearable Ubiquitous Technol.* 2, 3, Article 94 (Sept. 2018), 19 pages. <https://doi.org/10.1145/3264904>
- [4] William Buxton. 1990. A Three-State Model of Graphical Input. In *Proceedings of the IFIP TC13 Third International Conference on Human-Computer Interaction (INTERACT '90)*, North-Holland Publishing Co., NLD, 449–456.
- [5] Liwei Chan, Yi-Ling Chen, Chi-Hao Hsieh, Rong-Hao Liang, and Bing-Yu Chen. 2015. CyclopsRing: Enabling Whole-Hand and Context-Aware Interactions Through a Fisheye Ring. In *Proceedings of the 28th Annual ACM Symposium on User Interface Software and Technology* (Charlotte, NC, USA) (UIST '15). Association for Computing Machinery, New York, NY, USA, 549–556. <https://doi.org/10.1145/2807442.2807450>
- [6] Liwei Chan, Rong-Hao Liang, Ming-Chang Tsai, Kai-Yin Cheng, Chao-Huai Su, Mike Y. Chen, Wen-Huang Cheng, and Bing-Yu Chen. 2013. FingerPad: Private and Subtle Interaction Using Fingertips. In *Proceedings of the 26th Annual ACM Symposium on User Interface Software and Technology* (St. Andrews, Scotland, United Kingdom) (UIST '13). Association for Computing Machinery, New York, NY, USA, 255–260. <https://doi.org/10.1145/2501988.2502016>
- [7] Ke-Yu Chen, Shwetak N. Patel, and Sean Keller. 2016. Finexus: Tracking Precise Motions of Multiple Fingertips Using Magnetic Sensing. In *Proceedings of the 2016 CHI Conference on Human Factors in Computing Systems* (San Jose, California, USA) (CHI '16). Association for Computing Machinery, New York, NY, USA, 1504–1514. <https://doi.org/10.1145/2858036.2858125>
- [8] Paul Dietz and Darren Leigh. 2001. DiamondTouch: A Multi-User Touch Technology. In *Proceedings of the 14th Annual ACM Symposium on User Interface Software and Technology* (Orlando, Florida) (UIST '01). Association for Computing Machinery, New York, NY, USA, 219–226. <https://doi.org/10.1145/502348.502389>
- [9] Paul H. Dietz, Bret Harsham, Clifton Forlines, Darren Leigh, William Yerazunis, Sam Shipman, Bent Schmidt-Nielsen, and Kathy Ryall. 2005. DT Controls: Adding Identity to Physical Interfaces. In *Proceedings of the 18th Annual ACM Symposium on User Interface Software and Technology* (Seattle, WA, USA) (UIST '05). Association for Computing Machinery, New York, NY, USA, 245–252. <https://doi.org/10.1145/1095034.1095075>
- [10] Masaaki Fukumoto and Yasuhito Suenaga. 1994. “FingerRing”: A Full-Time Wearable Interface. In *Conference Companion on Human Factors in Computing Systems* (Boston, Massachusetts, USA) (CHI '94). Association for Computing Machinery, New York, NY, USA, 81–82. <https://doi.org/10.1145/259963.260056>
- [11] Masaaki Fukumoto and Yoshinobu Tonomura. 1997. “Body Coupled FingerRing”: Wireless Wearable Keyboard. In *Proceedings of the ACM SIGCHI Conference on Human Factors in Computing Systems* (Atlanta, Georgia, USA) (CHI '97). Association for Computing Machinery, New York, NY, USA, 147–154. <https://doi.org/10.1145/258549.258636>
- [12] Tobias Grosse-Puppenthal, Christian Holz, Gabe Cohn, Raphael Wimmer, Oskar Bechtold, Steve Hodges, Matthew S. Reynolds, and Joshua R. Smith. 2017. Finding Common Ground: A Survey of Capacitive Sensing in Human-Computer Interaction. In *Proceedings of the 2017 CHI Conference on Human Factors in Computing Systems* (Denver, Colorado, USA) (CHI '17). Association for Computing Machinery, New York, NY, USA, 3293–3315. <https://doi.org/10.1145/3025453.3025808>
- [13] Yizheng Gu, Chun Yu, Zhipeng Li, Weiqi Li, Shuchang Xu, Xiaoying Wei, and Yuanchun Shi. 2019. Accurate and Low-Latency Sensing of Touch Contact on Any Surface with Finger-Worn IMU Sensor. In *Proceedings of the 32nd Annual ACM Symposium on User Interface Software and Technology* (New Orleans, LA, USA) (UIST '19). Association for Computing Machinery, New York, NY, USA, 1059–1070. <https://doi.org/10.1145/3332165.3347947>
- [14] Aakar Gupta, Cheng Ji, Hui-Shyong Yeo, Aaron Quigley, and Daniel Vogel. 2019. RotoSwyype: Word-Gesture Typing Using a Ring. In *Proceedings of the 2019 CHI Conference on Human Factors in Computing Systems* (Glasgow, Scotland UK) (CHI '19). Association for Computing Machinery, New York, NY, USA, Article 14, 12 pages. <https://doi.org/10.1145/3290605.3300244>
- [15] Jefferson Y. Han. 2005. Low-Cost Multi-Touch Sensing through Frustrated Total Internal Reflection. In *Proceedings of the 18th Annual ACM Symposium on User Interface Software and Technology* (Seattle, WA, USA) (UIST '05). Association for Computing Machinery, New York, NY, USA, 115–118. <https://doi.org/10.1145/1095034.1095054>
- [16] Chris Harrison, Hrovje Benko, and Andrew D. Wilson. 2011. OmniTouch: Wearable Multitouch Interaction Everywhere. In *Proceedings of the 24th Annual ACM Symposium on User Interface Software and Technology* (Santa Barbara, California, USA) (UIST '11). Association for Computing Machinery, New York, NY, USA, 441–450. <https://doi.org/10.1145/2047196.2047255>
- [17] Chris Harrison, Desney Tan, and Dan Morris. 2010. Skinput: Appropriating the Body as an Input Surface. In *Proceedings of the SIGCHI Conference on Human Factors in Computing Systems* (Atlanta, Georgia, USA) (CHI '10). Association for Computing Machinery, New York, NY, USA, 453–462. <https://doi.org/10.1145/1753326.1753394>
- [18] Christian Holz and Marius Knaust. 2015. Biometric Touch Sensing: Seamlessly Augmenting Each Touch with Continuous Authentication. In *Proceedings of the 28th Annual ACM Symposium on User Interface Software and Technology* (Charlotte, NC, USA) (UIST '15). Association for Computing Machinery, New York, NY, USA, 303–312. <https://doi.org/10.1145/2807442.2807458>
- [19] Hsin-Liu (Cindy) Kao, Christian Holz, Asta Roseway, Andres Calvo, and Chris Schmandt. 2016. DuoSkin: Rapidly Prototyping on-Skin User Interfaces Using Skin-Friendly Materials. In *Proceedings of the 2016 ACM International Symposium on Wearable Computers* (Heidelberg, Germany) (ISWC '16). Association for Computing Machinery, New York, NY, USA, 16–23. <https://doi.org/10.1145/2971763.2971777>
- [20] Keiko Katsuragawa, Ju Wang, Ziyang Shan, Ningshan Ouyang, Omid Abari, and Daniel Vogel. 2019. Tip-Tap: Battery-Free Discrete 2D Fingertip Input. In *Proceedings of the 32nd Annual ACM Symposium on User Interface Software and Technology* (New Orleans, LA, USA) (UIST '19). Association for Computing Machinery, New York, NY, USA, 1045–1057. <https://doi.org/10.1145/3332165.3347907>
- [21] Wolf Kienzle and Ken Hinckley. 2014. LightRing: Always-Available 2D Input on Any Surface. In *Proceedings of the 27th Annual ACM Symposium on User Interface Software and Technology* (Honolulu, Hawaii, USA) (UIST '14). Association for Computing Machinery, New York, NY, USA, 157–160. <https://doi.org/10.1145/2642918.2647376>
- [22] David Kim, Otmarr Hilliges, Shahram Izadi, Alex D. Butler, Jiawen Chen, Iason Oikonomidis, and Patrick Olivier. 2012. Digits: Freehand 3D Interactions Anywhere Using a Wrist-Worn Gloveless Sensor. In *Proceedings of the 25th Annual ACM Symposium on User Interface Software and Technology* (Cambridge, Massachusetts, USA) (UIST '12). Association for Computing Machinery, New York, NY, USA, 167–176. <https://doi.org/10.1145/2380116.2380139>
- [23] Jihyun Lee, Byungmoon Kim, Bongwon Suh, and Eunye Koh. 2016. Exploring the Front Touch Interface for Virtual Reality Headsets. In *Proceedings of the 2016 CHI Conference Extended Abstracts on Human Factors in Computing Systems* (San Jose, California, USA) (CHI EA '16). Association for Computing Machinery, New York, NY, USA, 2585–2591. <https://doi.org/10.1145/2851581.2892344>
- [24] SK Lee, William Buxton, and K. C. Smith. 1985. A Multi-Touch Three Dimensional Touch-Sensitive Tablet. In *Proceedings of the SIGCHI Conference on Human Factors in Computing Systems* (San Francisco, California, USA) (CHI '85). Association for Computing Machinery, New York, NY, USA, 21–25. <https://doi.org/10.1145/317456.317461>
- [25] Kent Lyons. 2016. 2D Input for Virtual Reality Enclosures with Magnetic Field Sensing. In *Proceedings of the 2016 ACM International Symposium on Wearable Computers* (Heidelberg, Germany) (ISWC '16). Association for Computing Machinery, New York, NY, USA, 176–183. <https://doi.org/10.1145/2971763.2971787>
- [26] Nobuyuki Matsushita and Jun Rekimoto. 1997. HoloWall: Designing a Finger, Hand, Body, and Object Sensitive Wall. In *Proceedings of the 10th Annual ACM Symposium on User Interface Software and Technology* (Banff, Alberta, Canada) (UIST '97). Association for Computing Machinery, New York, NY, USA, 209–210. <https://doi.org/10.1145/263407.263549>
- [27] Adiyen Mujibiya, Xiang Cao, Desney S. Tan, Dan Morris, Shwetak N. Patel, and Jun Rekimoto. 2013. The Sound of Touch: On-Body Touch and Gesture Sensing Based on Transdermal Ultrasound Propagation. In *Proceedings of the 2013 ACM International Conference on Interactive Tabletops and Surfaces* (St. Andrews, Scotland, United Kingdom) (ITS '13). Association for Computing Machinery, New York, NY, USA, 189–198. <https://doi.org/10.1145/2512349.2512821>
- [28] Rajalakshmi Nandakumar, Vikram Iyer, Desney Tan, and Shyamnath Gollakota. 2016. FingerIO: Using Active Sonar for Fine-Grained Finger Tracking. In *Proceedings of the 2016 CHI Conference on Human Factors in Computing Systems* (San Jose, California, USA) (CHI '16). Association for Computing Machinery, New York, NY, USA, 1515–1525. <https://doi.org/10.1145/2858036.2858580>
- [29] Aditya Shekhar Nittala, Anusha Withana, Narjes Pourjafarian, and Jürgen Steimle. 2018. Multi-Touch Skin: A Thin and Flexible Multi-Touch Sensor for On-Skin Input. In *Proceedings of the 2018 CHI Conference on Human Factors in Computing Systems* (Montreal QC, Canada) (CHI '18). Association for Computing Machinery,

- New York, NY, USA, 1–12. <https://doi.org/10.1145/3173574.3173607>
- [30] Shijia Pan, Ceferino Gabriel Ramirez, Mostafa Mirshekari, Jonathon Fagert, Albert Jin Chung, Chih Chi Hu, John Paul Shen, Hae Young Noh, and Pei Zhang. 2017. SurfaceVibe: Vibration-Based Tap & Swipe Tracking on Ubiquitous Surfaces. In *Proceedings of the 16th ACM/IEEE International Conference on Information Processing in Sensor Networks* (Pittsburgh, Pennsylvania) (IPSN '17). Association for Computing Machinery, New York, NY, USA, 197–208. <https://doi.org/10.1145/3055031.3055077>
- [31] J. A. Paradiso, Che King Leo, N. Checka, and Kaijen Hsiao. 2002. Passive acoustic sensing for tracking knocks atop large interactive displays. In *SENSORS, 2002 IEEE*, Vol. 1. 521–527 vol.1.
- [32] Farshid Salemi Parizi, Eric Whitmire, and Shwetak Patel. 2019. AuraRing: Precise Electromagnetic Finger Tracking. *Proc. ACM Interact. Mob. Wearable Ubiquitous Technol.* 3, 4, Article 150 (Dec. 2019), 28 pages. <https://doi.org/10.1145/3369831>
- [33] Claudio S. Pinhanez. 2001. The Everywhere Displays Projector: A Device to Create Ubiquitous Graphical Interfaces. In *Proceedings of the 3rd International Conference on Ubiquitous Computing* (Atlanta, Georgia, USA) (UbiComp '01). Springer-Verlag, Berlin, Heidelberg, 315–331.
- [34] Ivan Poupyrev, Nan-Wei Gong, Shiho Fukuhara, Mustafa Emre Karagozler, Carsten Schwesig, and Karen E. Robinson. 2016. Project Jacquard: Interactive Digital Textiles at Scale. In *Proceedings of the 2016 CHI Conference on Human Factors in Computing Systems* (San Jose, California, USA) (CHI '16). Association for Computing Machinery, New York, NY, USA, 4216–4227. <https://doi.org/10.1145/2858036.2858176>
- [35] Ivan Poupyrev, Chris Harrison, and Munehiko Sato. 2012. Touché: Touch and Gesture Sensing for the Real World. In *Proceedings of the 2012 ACM Conference on Ubiquitous Computing* (Pittsburgh, Pennsylvania) (UbiComp '12). Association for Computing Machinery, New York, NY, USA, 536. <https://doi.org/10.1145/2370216.2370296>
- [36] Shanaka Ransiri, Roshan Lalintha Peiris, Kian Peen Yeo, and Suranga Nanayakkara. 2013. SmartFinger: Connecting Devices, Objects and People Seamlessly. In *Proceedings of the 25th Australian Computer-Human Interaction Conference: Augmentation, Application, Innovation, Collaboration* (Adelaide, Australia) (OzCHI '13). Association for Computing Machinery, New York, NY, USA, 359–362. <https://doi.org/10.1145/2541016.2541064>
- [37] Roy Shilkrot, Jochen Huber, Wong Meng Ee, Pattie Maes, and Suranga Chandima Nanayakkara. 2015. FingerReader: A Wearable Device to Explore Printed Text on the Go. In *Proceedings of the 33rd Annual ACM Conference on Human Factors in Computing Systems* (Seoul, Republic of Korea) (CHI '15). Association for Computing Machinery, New York, NY, USA, 2363–2372. <https://doi.org/10.1145/2702123.2702421>
- [38] Y. Song, Q. Hao, K. Zhang, M. Wang, Y. Chu, and B. Kang. 2011. The Simulation Method of the Galvanic Coupling Intrabody Communication With Different Signal Transmission Paths. *IEEE Transactions on Instrumentation and Measurement* 60, 4 (2011), 1257–1266.
- [39] Virag Varga. 2019. *Reinventing Touch with Body Channel Communication - System Design from Electric Fields To Mixed Reality*. Ph.D. Dissertation. ETH Zurich, Zurich. <https://doi.org/10.3929/ethz-b-000356345>
- [40] Virag Varga, Gergely Vakulya, Alanson Sample, and Thomas R. Gross. 2018. Enabling Interactive Infrastructure with Body Channel Communication. *Proc. ACM Interact. Mob. Wearable Ubiquitous Technol.* 1, 4, Article 169 (Jan. 2018), 29 pages. <https://doi.org/10.1145/3161180>
- [41] Virag Varga, Marc Wyss, Gergely Vakulya, Alanson Sample, and Thomas R. Gross. 2018. Designing Groundless Body Channel Communication Systems: Performance and Implications. In *Proceedings of the 31st Annual ACM Symposium on User Interface Software and Technology* (Berlin, Germany) (UIST '18). Association for Computing Machinery, New York, NY, USA, 683–695. <https://doi.org/10.1145/3242587.3242622>
- [42] Edward Jay Wang, Jake Garrison, Eric Whitmire, Mayank Goel, and Shwetak Patel. 2017. Carpacio: Repurposing Capacitive Sensors to Distinguish Driver and Passenger Touches on In-Vehicle Screens. In *Proceedings of the 30th Annual ACM Symposium on User Interface Software and Technology* (Québec City, QC, Canada) (UIST '17). Association for Computing Machinery, New York, NY, USA, 49–55. <https://doi.org/10.1145/3126594.3126623>
- [43] Martin Weigel, Tong Lu, Gilles Bailly, Antti Oulasvirta, Carmel Majidi, and Jürgen Steimle. 2015. ISkin: Flexible, Stretchable and Visually Customizable On-Body Touch Sensors for Mobile Computing. In *Proceedings of the 33rd Annual ACM Conference on Human Factors in Computing Systems* (Seoul, Republic of Korea) (CHI '15). Association for Computing Machinery, New York, NY, USA, 2991–3000. <https://doi.org/10.1145/2702123.2702391>
- [44] Andrew D. Wilson and Hrvoje Benko. 2010. Combining Multiple Depth Cameras and Projectors for Interactions on, above and between Surfaces. In *Proceedings of the 23rd Annual ACM Symposium on User Interface Software and Technology* (New York, New York, USA) (UIST '10). Association for Computing Machinery, New York, NY, USA, 273–282. <https://doi.org/10.1145/1866029.1866073>
- [45] Robert Xiao, Julia Schwarz, Nick Throm, Andrew D. Wilson, and Hrvoje Benko. 2018. MRTouch: Adding Touch Input to Head-Mounted Mixed Reality. *IEEE Transactions on Visualization and Computer Graphics* 24, 4 (April 2018), 1653–1660. <https://doi.org/10.1109/TVCG.2018.2794222>
- [46] Zheer Xu, Pui Chung Wong, Jun Gong, Te-Yen Wu, Aditya Shekhar Nittala, Xiaojun Bi, Jürgen Steimle, Hongbo Fu, Kening Zhu, and Xing-Dong Yang. 2019. TipText: Eyes-Free Text Entry on a Fingertip Keyboard. In *Proceedings of the 32nd Annual ACM Symposium on User Interface Software and Technology* (New Orleans, LA, USA) (UIST '19). Association for Computing Machinery, New York, NY, USA, 883–899. <https://doi.org/10.1145/3332165.3347865>
- [47] Xing-Dong Yang, Tovi Grossman, Daniel Wigdor, and George Fitzmaurice. 2012. Magic Finger: Always-Available Input through Finger Instrumentation. In *Proceedings of the 25th Annual ACM Symposium on User Interface Software and Technology* (Cambridge, Massachusetts, USA) (UIST '12). Association for Computing Machinery, New York, NY, USA, 147–156. <https://doi.org/10.1145/2380116.2380137>
- [48] Hui-Shyong Yeo, Juyoung Lee, Hyung-il Kim, Aakar Gupta, Andrea Bianchi, Daniel Vogel, Hideki Koike, Woontack Woo, and Aaron Quigley. 2019. WRIST: Watch-Ring Interaction and Sensing Technique for Wrist Gestures and Macro-Micro Pointing. In *Proceedings of the 21st International Conference on Human-Computer Interaction with Mobile Devices and Services* (Taipei, Taiwan) (MobileHCI '19). Association for Computing Machinery, New York, NY, USA, Article 19, 15 pages. <https://doi.org/10.1145/3338286.3340130>
- [49] Sang Ho Yoon, Ke Huo, Yunbo Zhang, Guiming Chen, Luis Paredes, Subramanian Chidambaram, and Karthik Ramani. 2017. ISoft: A Customizable Soft Sensor with Real-Time Continuous Contact and Stretching Sensing. In *Proceedings of the 30th Annual ACM Symposium on User Interface Software and Technology* (Québec City, QC, Canada) (UIST '17). Association for Computing Machinery, New York, NY, USA, 665–678. <https://doi.org/10.1145/3126594.3126654>
- [50] Cheng Zhang, Abdelkareem Bedri, Gabriel Reyes, Bailey Berck, Omer T. Inan, Thad E. Starner, and Gregory D. Abowd. 2016. TapSkin: Recognizing On-Skin Input for Smartwatches. In *Proceedings of the 2016 ACM International Conference on Interactive Surfaces and Spaces* (Niagara Falls, Ontario, Canada) (ISS '16). Association for Computing Machinery, New York, NY, USA, 13–22. <https://doi.org/10.1145/2992154.2992187>
- [51] Yang Zhang and Chris Harrison. 2018. Pulp Nonfiction: Low-Cost Touch Tracking for Paper. In *Proceedings of the 2018 CHI Conference on Human Factors in Computing Systems* (Montreal QC, Canada) (CHI '18). Association for Computing Machinery, New York, NY, USA, 1–11. <https://doi.org/10.1145/3173574.3173691>
- [52] Yang Zhang, Wolf Kienzle, Yanjun Ma, Shiu S. Ng, Hrvoje Benko, and Chris Harrison. 2019. ActiTouch: Robust Touch Detection for On-Skin AR/VR Interfaces. In *Proceedings of the 32nd Annual ACM Symposium on User Interface Software and Technology* (New Orleans, LA, USA) (UIST '19). Association for Computing Machinery, New York, NY, USA, 1151–1159. <https://doi.org/10.1145/3332165.3347869>
- [53] Yang Zhang, Gierad Laput, and Chris Harrison. 2017. Electrck: Low-Cost Touch Sensing Using Electric Field Tomography. In *Proceedings of the 2017 CHI Conference on Human Factors in Computing Systems* (Denver, Colorado, USA) (CHI '17). Association for Computing Machinery, New York, NY, USA, 1–14. <https://doi.org/10.1145/3025453.3025842>
- [54] Yang Zhang, Chouchang (Jack) Yang, Scott E. Hudson, Chris Harrison, and Alanson Sample. 2018. Wall++: Room-Scale Interactive and Context-Aware Sensing. In *Proceedings of the 2018 CHI Conference on Human Factors in Computing Systems* (Montreal QC, Canada) (CHI '18). Association for Computing Machinery, New York, NY, USA, 1–15. <https://doi.org/10.1145/3173574.3173847>
- [55] Yang Zhang, Junhan Zhou, Gierad Laput, and Chris Harrison. 2016. SkinTrack: Using the Body as an Electrical Waveguide for Continuous Finger Tracking on the Skin. In *Proceedings of the 2016 CHI Conference on Human Factors in Computing Systems* (San Jose, California, USA) (CHI '16). Association for Computing Machinery, New York, NY, USA, 1491–1503. <https://doi.org/10.1145/2858036.2858082>

A APPENDIX

To enable replication of this work, we provide schematics for both the transmit driver and receiver front end. ElectroRing uses a PSoc 6 to sample the AC signal and extract the frequency of interest, but another suitable SoC or MCU with external ADC would be appropriate to use as well.

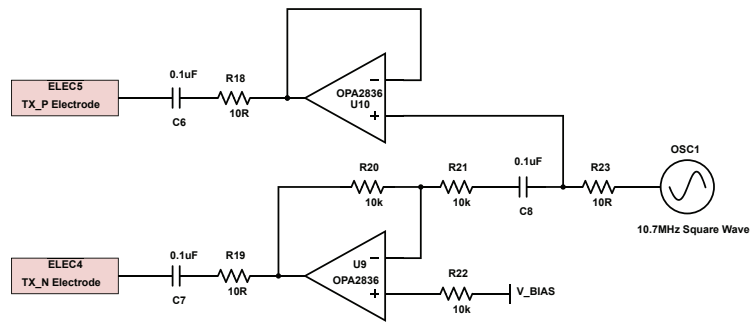


Figure 11: Schematic diagram of ElectroRing transmit driver.

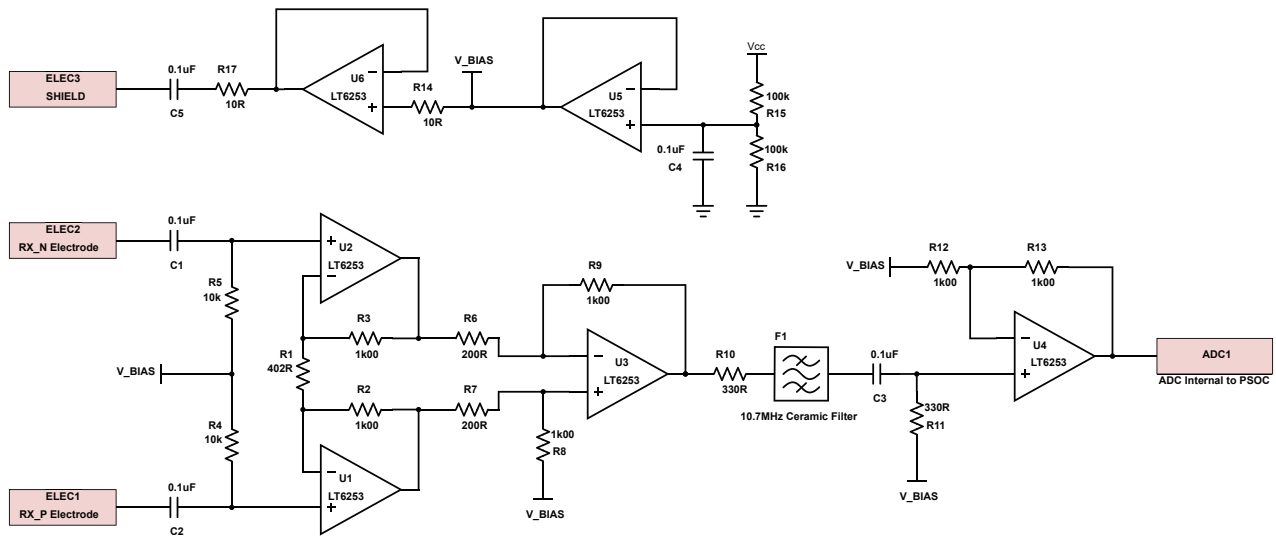


Figure 12: Schematic diagram of ElectroRing receiver analog front end. The shield electrode is biased at the half rail voltage.